 CMES, vol.56, no.1, pp.17-40, 2010

A High-Order Time and Space Formulation of the Unsplit Perfectly Matched Layer for the Seismic Wave Equation Using Auxiliary Differential Equations (ADE-PML)

R. Martin[1], **D. Komatitsch**[1,2], **S. D. Gedney**[3] **and E. Bruthiaux**[1,4]

Abstract: Unsplit convolutional perfectly matched layers (CPML) for the velocity and stress formulation of the seismic wave equation are classically computed based on a second-order finite-difference time scheme. However it is often of interest to increase the order of the time-stepping scheme in order to increase the accuracy of the algorithm. This is important for instance in the case of very long simulations. We study how to define and implement a new unsplit non-convolutional PML called the Auxiliary Differential Equation PML (ADE-PML), based on a high-order Runge-Kutta time-stepping scheme and optimized at grazing incidence. We demonstrate that when a second-order time-stepping scheme is used the convolutional PML can be derived from that more general non-convolutional ADE-PML formulation, but that this new approach can be generalized to high-order schemes in time, which implies that it can be made more accurate. We also show that the ADE-PML formulation is numerically stable up to 100,000 time steps.

Keywords: Finite differences, FDTD, high-order, Perfectly Matched Layer (PML), seismic wave propagation, absorbing conditions, Auxiliary Differential Equations (ADE).

1 Introduction

Several numerical techniques can be used to model seismic wave propagation, for instance the finite-difference (FD) method (e.g., Madariaga, 1976), spectral

[1] Université de Pau et des Pays de l'Adour, CNRS and INRIA Magique-3D. Laboratoire de Modélisation et Imagerie en Géosciences UMR 5212, Avenue de l'Université, 64013 Pau cedex, France. E-mail: roland.martin@univ-pau.fr, dimitri.komatitsch@univ-pau.fr

[2] Institut universitaire de France, 103 boulevard Saint-Michel, 75005 Paris, France

[3] Department of Electrical and Computer Engineering, University of Kentucky, Lexington, KY 40506-0046, USA. E-mail: gedney@engr.uky.edu

[4] École Normale Supérieure de Lyon, Laboratoire de Sciences de la Terre, UMR 5570, 46 allée d'Italie, 69007 Lyon, France. E-mail: emilien.bruthiaux@ens-lyon.fr

or pseudo-spectral techniques (Tessmer and Kosloff, 1994; Komatitsch, Coutel, and Mora, 1996), boundary-element or boundary-integral methods (Kawase, 1988; Sánchez-Sesma and Campillo, 1991; Rodríguez-Castellanos, Sánchez-Sesma, Luzón, and Martin, 2006), finite-element methods (Lysmer and Drake, 1972) or spectral-element methods (Liu, Polet, Komatitsch, and Tromp, 2004; Chaljub, Komatitsch, Vilotte, Capdeville, Valette, and Festa, 2007; Tromp, Komatitsch, and Liu, 2008). In order to mimic an infinite or semi-infinite medium, absorbing techniques have been developed and adapted to the above mentioned methods: for instance damping layers or 'sponge zones' (Cerjan, Kosloff, Kosloff, and Reshef, 1985; Sochacki, Kubichek, George, Fletcher, and Smithson, 1987), paraxial conditions (Engquist and Majda, 1977; Stacey, 1988; Higdon, 1991) or asymptotic local or non-local high-order operators (Givoli, 1991, 2008; Hagstrom and Hariharan, 1998).

The Perfectly Matched Layer (PML), introduced by Bérenger (1994) for Maxwell's equations, is now widely used because it has the advantage of having a zero reflection coefficient at all angles of incidence and at all frequencies before discretization by a numerical scheme in the case of an infinite PML. It was rapidly reformulated with complex coordinate stretching for a split wave field (Chew and Weedon, 1994; Collino and Monk, 1998) and applied to acoustic or elastic problems (Chew and Liu, 1996; Collino and Tsogka, 2001; Komatitsch and Tromp, 2003; Fauqueux, 2003; Marcinkovich and Olsen, 2003; Wang and Tang, 2003; Basu and Chopra, 2004; Cohen and Fauqueux, 2005; Festa and Vilotte, 2005; Ma and Liu, 2006; Lu and Zhu, 2007; Komatitsch and Martin, 2007; Basu, 2009; Kristek, Moczo, and Galis, 2009) as well as to viscoelastic (Martin and Komatitsch, 2009) or poroelastic (Zeng, He, and Liu, 2001; Martin, Komatitsch, and Ezziani, 2008) media.

In the context of finite-difference formulations of the classical PML, the seismic wave equation is usually written as a first-order velocity-stress system in time. That first-order formulation can not be used as such in second-order displacement formulations such as finite-element methods, spectral-element methods or some finite-difference methods (Moczo, Robertsson, and Eisner, 2007). Komatitsch and Tromp (2003) and Basu and Chopra (2004) derived PML formulations suitable for the second-order system written in displacement. Festa and Vilotte (2005) showed that the first-order PML formulation can be used together with a second-order formulation of the equations inside the computational domain because the Newmark time-stepping scheme and the midpoint rule used in the staggered velocity-stress formulation are equivalent. Even if the PML is perfectly matched by construction before discretization, after discretization it is no longer perfectly matched, which generates spurious waves that propagate back into the main domain. This is accentuated for waves reaching the PML layer at grazing incidence. To overcome these problems, one can modify the complex coordinate stretching used classically

in the PML by introducing a shifting of the poles and implementing a Butterworth-like filter in the PML (Kuzuoglu and Mittra, 1996). This has first been developed for Maxwell's equation (Roden and Gedney, 2000; Bérenger, 2002a,b) and then adapted to the seismic wave equation in the context of unsplit 2D or 3D finite-difference formulations (Martin, Komatitsch, and Barucq, 2005; Martin and Komatitsch, 2006; Komatitsch and Martin, 2007; Drossaert and Giannopoulos, 2007; Martin, Komatitsch, and Ezziani, 2008), or a split 2D spectral-element formulation (Festa and Vilotte, 2005; Festa, Delavaud, and Vilotte, 2005).

Meza-Fajardo and Papageorgiou (2008) suggested a sponge layer called the Multiaxial PML (M-PML) based on a stabilization of a split PML formulation. It is not a PML any more because by coupling two damping directions the perfectly matched layer character of the technique of Bérenger (1994) is lost (the theoretical reflection coefficient for an infinite PML is not exactly zero any more before discretization). An unsplit variational formulation has been proposed in the context of the spectral-element technique in Martin, Komatitsch, and Gedney (2008). In Komatitsch and Martin (2007) and Martin, Komatitsch, and Ezziani (2008) seismic wave propagation was modeled based on numerical schemes that are second-order in time and space. For wave propagation in viscoelastic and poroelastic media, in Martin, Komatitsch, and Ezziani (2008) and Martin and Komatitsch (2009) we used a fourth-order spatial scheme but kept a second-order time-stepping scheme. But many authors use finite differences at high order in both space and time (see e.g. Dablain (1986)) for real applications to increase accuracy and reduce the numerical cost, in particular for long simulations. It is thus important to be able to extend the CPML to higher-order time schemes.

Therefore in this article we design a PML improved at grazing incidence based on a fourth-order Runge-Kutta time-stepping scheme and an eighth-order scheme in space. We use some ideas coming from the high-order PML formulation developed for Maxwell's equations by Gedney and Zhao (2010) and apply them to seismic wave propagation. The main idea is to notice that the time stepping formulation of the auxiliary memory variables arising from the second-order trapezoidal integration rule applied to the time discretization of the convolution term can be reformulated in a similar form that can be interpreted as a time-evolution equation for the memory variables. That formulation is called ADE-PML (Gedney and Zhao, 2010), that is to say a PML using an Auxiliary Differential Equation. These memory variable equations together with the equations of time evolution of the velocity and stress components can be used with stretching functions with more than one pole in the PML frequency shift, thus implementing a Butterworth filter to improve the behavior at grazing incidence as in the CPML. In this article, we validate the approach by comparing seismograms to a high-order FD reference solution cal-

culated on a large domain, and we study the accuracy and stability for long time periods numerically.

2 Equivalence between convolution and ADE (auxiliary differential equations) perfectly matched layers

Let us compare different formulations and discretizations of the elastodynamics equation and show the equivalence between CPML and the non-convolutional ADE-PML for a second-order time discretization. This will also allow the derivation of the high-order time-advancement scheme of the ADE-PML.

The elastodynamics equation written as a first-order system in velocity vector and stress tensor is (e.g., Madariaga, 1976; Virieux, 1986; Moczo, Robertsson, and Eisner, 2007):

$$\begin{aligned} \rho \frac{\partial v_i}{\partial t} &= \frac{\partial \sigma_{ij}}{\partial x_j} + s_i \\ \frac{\partial \sigma_{ij}}{\partial t} &= \lambda \varepsilon_{kk} \delta_{ij} + 2\mu \varepsilon_{ij}, \end{aligned} \tag{1}$$

where $\varepsilon_{ij} = \frac{1}{2}\left(\frac{\partial v_j}{\partial x_i} + \frac{\partial v_i}{\partial x_j}\right)$ is the velocity strain tensor, v_i are the components of the velocity vector, σ_{ij} the components of the stress tensor, s_i are the components of the (known) source force vector, ρ is the density and λ and μ are the Lamé parameters. In two dimensions we can develop the equations as

$$\begin{aligned} \rho \frac{\partial v_x}{\partial t} &= \frac{\partial \sigma_{xx}}{\partial x} + \frac{\partial \sigma_{xy}}{\partial y} + s_x \\ \rho \frac{\partial v_y}{\partial t} &= \frac{\partial \sigma_{xy}}{\partial x} + \frac{\partial \sigma_{yy}}{\partial y} + s_y \\ \frac{\partial \sigma_{xx}}{\partial t} &= (\lambda + 2\mu) \frac{\partial v_x}{\partial x} + \lambda \frac{\partial v_y}{\partial y} \\ \frac{\partial \sigma_{yy}}{\partial t} &= (\lambda + 2\mu) \frac{\partial v_y}{\partial y} + \lambda \frac{\partial v_x}{\partial x} \\ \frac{\partial \sigma_{xy}}{\partial t} &= \mu \left(\frac{\partial v_x}{\partial y} + \frac{\partial v_y}{\partial x} \right). \end{aligned} \tag{2}$$

In our previous articles on the unsplit perfectly matched layer formulation we performed a convolution integration of the memory variable equations following Luebbers and Hunsberger (1992). But let us show that a simple time advancing equation of the memory variables can be formulated and discretized using a high-order semi-implicit time scheme. As in the construction of a classical PML or a Convolution

PML, the spatial derivatives along the axis perpendicular to the PML layer, say x, are rewritten in a stretched coordinate $\tilde{x}$, based on (see e.g. Komatitsch and Martin (2007)):

$$\partial_{\tilde{x}} = \frac{1}{s_x}\partial_x \tag{3}$$

where

$$s_x = \kappa_x + \frac{d_x}{\alpha_x + i\omega}. \tag{4}$$

Then, following Komatitsch and Martin (2007), we can express:

$$\frac{1}{s_x} = \frac{1}{\kappa_x} - \frac{d_x}{\kappa_x^2}\frac{1}{(d_x/\kappa_x + \alpha_x) + i\omega} \tag{5}$$

and

$$\begin{aligned} d_x &= d_0\left(\frac{x}{L}\right)^N \\ \kappa_x &= 1 + (\kappa_{\max} - 1)^m \\ \alpha_x &= \alpha_{\max}[1 - (x/L)^p] \end{aligned} \tag{6}$$

where L is the thickness of the PML layer, $N = 2$ and $d_0 = -\frac{(N+1)c_{pmax}\log(R_c)}{2L}$, c_{pmax} being equal to the speed of the pressure wave and R_c being the target theoretical reflection coefficient, chosen here as 0.1% (see e.g. Collino and Tsogka (2001)). We also take $p = 1$ and $\alpha_{\max} = \pi f_0$, where f_0 is the dominant frequency of the seismic source. $\kappa_{\max}$ usually lies between 1 and 20 (Martin and Komatitsch, 2009) and we usually take $m = 2$. By sake of simplicity we will study the term $\partial_x\sigma_{xy}$ in detail, keeping in mind that similar formulations are derived for the x and y derivatives of v_x, v_y, σ_{xx} and σ_{yy} in 2D when PML layers are present along both axes of the grid. The term $\partial_x\sigma_{xy}$ is transformed into

$$\frac{1}{s_x}\partial_x\sigma_{xy} = \frac{1}{\kappa_x}\partial_x\sigma_{xy} - \frac{d_x}{\kappa_x^2}\frac{1}{(d_x/\kappa_x + \alpha_x) + i\omega}\partial_x\sigma_{xy}. \tag{7}$$

Let us denote $Q_x^{\sigma_{xy}}$ the auxiliary memory variable associated with $\partial_x\sigma_{xy}$, i.e.:

$$Q_x^{\sigma_{xy}} = -\frac{d_x}{\kappa_x^2}\frac{1}{(d_x/\kappa_x + \alpha_x) + i\omega}\partial_x\sigma_{xy}\,, \tag{8}$$

which leads to

$$\left(\frac{d_x}{\kappa_x} + \alpha_x + i\omega\right)Q_x^{\sigma_{xy}} = -\frac{d_x}{\kappa_x^2}\partial_x\sigma_{xy}. \tag{9}$$

Written in the time domain this equation becomes

$$\partial_t Q_x^{\sigma_{xy}} + \left(\frac{d_x}{\kappa_x} + \alpha_x \right) Q_x^{\sigma_{xy}} = -\frac{d_x}{\kappa_x^2} \partial_x \sigma_{xy} \tag{10}$$

and consequently the whole system of equations for elastodynamics with ADE-PML is

$$\begin{aligned}
\partial_t \sigma_{xx} &= (\lambda + 2\mu)(\frac{1}{\kappa_x}\partial_x v_x + Q_x^{v_x}) + \lambda(\frac{1}{\kappa_y}\partial_y v_y + Q_y^{v_y}) \\
\partial_t \sigma_{yy} &= (\lambda + 2\mu)(\frac{1}{\kappa_y}\partial_y v_y + Q_y^{v_y}) + \lambda(\frac{1}{\kappa_x}\partial_x v_x + Q_x^{v_x}) \\
\partial_t \sigma_{xy} &= \mu \left((\frac{1}{\kappa_x}\partial_x v_y + Q_x^{v_y}) + (\frac{1}{\kappa_y}\partial_y v_x + Q_y^{v_x}) \right) \\
\rho \partial_t v_x &= \frac{1}{\kappa_x}\partial_x \sigma_{xx} + Q_x^{\sigma_{xx}} + \frac{1}{\kappa_y}\partial_y \sigma_{xy} + Q_y^{\sigma_{xy}} \\
\rho \partial_t v_y &= \frac{1}{\kappa_x}\partial_x \sigma_{xy} + Q_x^{\sigma_{xy}} + \frac{1}{\kappa_y}\partial_y \sigma_{yy} + Q_y^{\sigma_{yy}} .
\end{aligned} \tag{11}$$

Let us now discretize the differential equations, taking the example of $Q_x^{\sigma_{xy}}$ again. Let us write

$$\partial_t Q_x^{\sigma_{xy}} + \frac{1}{\tau_x} Q_x^{\sigma_{xy}} = -\frac{d_x}{\kappa_x^2} \partial_x \sigma_{xy}, \tag{12}$$

where $\tau_x = \frac{1}{\frac{d_x}{\kappa_x} + \alpha_x}$. At time $t = -\infty$, the medium is at rest and contains no waves therefore we have $Q_x^{\sigma_{xy}}(-\infty) = \partial_t Q_x^{\sigma_{xy}}(-\infty) = 0$ and thus $\tau_x \frac{d_x}{\kappa_x^2} \partial_x \sigma_{xy} = 0$ at $t = -\infty$, which is relevant because there is no signal and thus velocities and stresses are equal to zero at $t = -\infty$. The solution of equation (12) can be formulated by the method of variable decomposition as

$$Q_x^{\sigma_{xy}} = A(x,y,t) \exp^{-\frac{t}{\tau_x}} . \tag{13}$$

At time $t = t^n$ we have

$$Q_x^{\sigma_{xy}}(t^n) = A(x,y,t^n) \exp^{-\frac{t^n}{\tau_x}} = A(x,y,t^n) \exp^{-\frac{t^{n-1}}{\tau_x}} \exp^{-\frac{\Delta t}{\tau_x}} . \tag{14}$$

By introducing equation (13) in equation (12) we obtain

$$\partial_t A(x,y,t) = -\frac{d_x}{\kappa_x^2} \exp^{\frac{t}{\tau_x}} \partial_x \sigma_{xy}. \tag{15}$$

Integrating this equation in time from t^{n-1} to t^n, we can write at second order in time

$$A(x,y,t^n) = A(x,y,t^{n-1}) - \tau_x \frac{d_x}{\kappa_x^2} \partial_x \sigma_{xy}^{n-1/2} \exp^{\frac{t^{n-1}}{\tau_x}} \times (\exp^{\frac{\Delta t}{\tau_x}} - 1) \tag{16}$$

and then, using equations (14) and (16), the time discretization of equation (12) at the second order in time reduces to

$$Q_x^{\sigma_{xy}}(t^n) = \exp^{-\frac{\Delta t}{\tau_x}} Q_x^{\sigma_{xy}}(t^{n-1}) - \tau_x \frac{d_x}{\kappa_x^2} (1 - \exp^{-\frac{\Delta t}{\tau_x}}) \partial_x \sigma_{xy}^{n-1/2}. \tag{17}$$

Finally we have

$$Q_x^{\sigma_{xy}}(t^n) = b_x Q_x^{\sigma_{xy}}(t^{n-1}) - a_x \frac{\partial \sigma_{xy}}{\partial x}^{n-1/2}, \tag{18}$$

where $b_x = \exp^{-\Delta t/\tau_x}$ and $a_x = \tau_x \frac{d_x}{\kappa_x^2}(1 - b_x)$.

One can notice that equation (18) has the same form as the CPML formulation of equation (26) of Komatitsch and Martin (2007), which shows that the CPML can be derived from the Auxiliary Differential Equation (ADE) formulation of equation (12) after time discretization when a second-order time scheme is used. The CPML can be seen as a particular case of the ADE-PML at the second order in time. But the advantage of the ADE-PML formulation is that it can be extended to a higher-order time scheme, as will be shown in Section 3.

3 High-order discretization in time and space of the non-convolutional ADE-PML formulation

Using a generalization of the equivalent ADE-PML equations, we can discretize the memory variable equations with higher accuracy based on a fourth-order Runge-Kutta (RK4) time scheme. A RK4 scheme in time consists of a four-step inner loop at each time step. At each step of the Runge-Kutta time scheme an explicit, semi-implicit or implicit treatment of the Q memory terms can be performed. In what follows, we first describe the time discretization of auxiliary memory variables in a generalized two-pole CPML formulation for one iteration, and second we describe the two-pole ADE-PML formulation for one iteration of the RK4 time scheme. We will see that in the frequency domain formulation the spatial derivatives are transformed identically in CPML and ADE-PML, and that the CPML and ADE-PML differ only after inverse Fourier transform in the time domain.

In equations (12) and (18) the C-PML or ADE-PML formulations are only filtered by one pole in the frequency shift of equation (2). Let us then introduce a more

general shift with two poles, i.e., a sharper (more accurate) Butterworth filter. Let us use the decomposition

$$\frac{1}{s_x} = \frac{1}{s_{x_1}} \frac{1}{s_{x_2}} \tag{19}$$

and let us denote the previous expression

$$\frac{1}{s} = \frac{1}{s_1} \frac{1}{s_2} \tag{20}$$

for simplicity. One can switch from CPML to ADE-PML by simply changing the coefficients involved in the calculation of memory variables after time discretization. At each time step, the auxiliary memory variables in the CPML formulation with two poles are computed at the second order using a similar technique as for the one-pole CPML version. Let us summarize the different steps in the case of two poles.

In the frequency domain we replace the derivative $\frac{\partial \sigma_{xy}}{\partial x}$ with $\frac{1}{s_1 s_2} \frac{\partial \sigma_{xy}}{\partial x}$, where

$$\frac{1}{s_1} \frac{1}{s_2} = \left(\frac{1}{\kappa_1} - \frac{1}{B_1} \right) \left(\frac{1}{\kappa_2} - \frac{1}{B_2} \right) = \left(\frac{1}{\kappa_1 \kappa_2} - \frac{1}{C_1} - \frac{1}{C_2} \right). \tag{21}$$

If we let

$$\begin{aligned} \frac{1}{B_1} &= -\frac{d_1}{\kappa_1^2 [(d_1/\kappa_1 + \alpha_1) + i\omega]} \\ \frac{1}{B_2} &= -\frac{d_2}{\kappa_2^2 [(d_2/\kappa_2 + \alpha_2) + i\omega]} \end{aligned} \tag{22}$$

then

$$\begin{aligned} \frac{1}{C_1} &= \frac{1}{\kappa_2 B_1} g_1 \\ \frac{1}{C_2} &= \frac{1}{\kappa_1 B_2} g_2 \end{aligned} \tag{23}$$

with

$$\begin{aligned} g_1 &= 1 - \frac{\kappa_1 d_2}{\xi_{1,2}} \\ g_2 &= 1 + \frac{\kappa_2 d_1}{\xi_{1,2}} \end{aligned} \tag{24}$$

and

$$\xi_{1,2} = \kappa_1(\kappa_2\alpha_2 + d_2) - \kappa_2(\kappa_1\alpha_1 + d_1). \tag{25}$$

Going back to the time domain by inverse Fourier transform and applying the recursive convolution as in the case of one pole, the derivative $\frac{1}{s_1}\frac{1}{s_2}\frac{\partial \sigma_{xy}}{\partial x}$ becomes $\frac{1}{\kappa_1\kappa_2}\frac{\partial \sigma_{xy}}{\partial x} + Q_1^{\sigma_{xy}} + Q_2^{\sigma_{xy}}$ in the CPML formulation, where

$$\begin{aligned} Q_1^{\sigma_{xy}}(n\Delta t) &= b_1 Q_1^{\sigma_{xy}}((n-1)\Delta t) - c_1 \frac{\partial \sigma_{xy}}{\partial x}^{n-1/2} \\ Q_2^{\sigma_{xy}}(n\Delta t) &= b_2 Q_2^{\sigma_{xy}}((n-1)\Delta t) - c_2 \frac{\partial \sigma_{xy}}{\partial x}^{n-1/2} \end{aligned} \tag{26}$$

and

$$\begin{aligned} b_1 &= \exp^{-\Delta t/\tau_1} \\ c_1 &= \alpha_1 \frac{g_1}{\kappa_2}(1-b_1) \\ b_2 &= \exp^{-\Delta t/\tau_2} \\ c_2 &= \alpha_2 \frac{g_2}{\kappa_1}(1-b_2). \end{aligned} \tag{27}$$

Here $\tau_i = \frac{1}{\frac{d_i}{\kappa_i}+\alpha_i}$ with $i = 1,2$. In practice we take $d_1 = d_2 = d_x$. If we want to use only one pole we set $s_2 = 1$ ($\kappa_2 = 1$ and $Q_2^{\sigma_{xy}} = 0$), which then gives the CPML formulation of equation (18). But we have seen above that the CPML formulation is not suitable at high order in time, therefore the equivalent ADE-PML formulation is preferred.

For the ADE-PML formulation with two poles we can apply the same reasoning as for the CPML. In the frequency domain $\frac{1}{s_1}\frac{1}{s_2}\frac{\partial \sigma_{xy}}{\partial x}$ becomes $\frac{1}{\kappa_1\kappa_2}\frac{\partial \sigma_{xy}}{\partial x} - \frac{1}{C_1}\partial_x\sigma_{xy} - \frac{1}{C_2}\partial_x\sigma_{xy}$ using equation (21). We introduce the auxiliary memory variables $Q_1^{\sigma_{xy}}$ and $Q_2^{\sigma_{xy}}$ defined as

$$Q_i^{\sigma_{xy}} = -\frac{1}{C_i}\partial_x\sigma_{xy} \tag{28}$$

for $i = 1,2$ and then

$$\begin{aligned} Q_1^{\sigma_{xy}} &= -\frac{1}{\kappa_2 B_1} g_1 \partial_x \sigma_{xy} \\ Q_2^{\sigma_{xy}} &= -\frac{1}{\kappa_1 B_2} g_2 \partial_x \sigma_{xy}. \end{aligned} \tag{29}$$

We then go back to the time domain by inverse Fourier transform and obtain the new formulation of derivatives $\frac{1}{\kappa_1\kappa_2}\frac{\partial\sigma_{xy}}{\partial x}+Q_1^{\sigma_{xy}}+Q_2^{\sigma_{xy}}$ with the following time evolution equations of the memory variables

$$\begin{aligned}\partial_t Q_1^{\sigma_{xy}}+\left(\frac{d_1}{\kappa_1}+\alpha_1\right)Q_1^{\sigma_{xy}} &= -\frac{d_1}{\kappa_1^2\kappa_2}g_1\partial_x\sigma_{xy}\\ \partial_t Q_2^{\sigma_{xy}}+\left(\frac{d_2}{\kappa_2}+\alpha_2\right)Q_2^{\sigma_{xy}} &= -\frac{d_2}{\kappa_2^2\kappa_1}g_2\partial_x\sigma_{xy}.\end{aligned} \tag{30}$$

where g_1 and g_2 are the functions defined in equations (24), i.e., the same functions as in the CPML formulation. After discretization of equation (30) in the time domain at the fourth order using RK4 time scheme, $Q_1^{\sigma_{xy}}$ satisfies

$$\begin{aligned}\frac{Q_1^{\sigma_{xy}}((n+\nu_i)\Delta t)-Q_1^{\sigma_{xy}}(n\Delta t)}{\nu_i\Delta t} &= -\frac{d_1}{\kappa_1^2\kappa_2}g_1\partial_x\sigma_{xy}((n+\nu_{i-1})\Delta t)\\ &\quad-\left(\frac{d_1}{\kappa_1}+\alpha_1\right)\left(\theta Q_1^{\sigma_{xy}}((n+\nu_i)\Delta t)+(1-\theta)Q_1^{\sigma_{xy}}(n\Delta t)\right).\end{aligned} \tag{31}$$

Finally we have

$$Q_1^{\sigma_{xy}}((n+\nu_i)\Delta t) = b_{1,i}Q_1^{\sigma_{xy}}(n\Delta t)-c_{1,i}\partial_x\sigma_{xy}((n+\nu_i)\Delta t) \tag{32}$$

with

$$b_{1,i} = \frac{\kappa_1-\theta\Delta t\nu_i(d_1+\kappa_1\alpha_1)}{\kappa_1+\theta\Delta t\nu_i(d_1+\kappa_1\alpha_1)} \tag{33}$$

$$c_{1,i} = -d_1g_1\frac{\Delta t\nu_i}{\kappa_1\kappa_2(\kappa_1+\theta\Delta t\nu_i(d_1+\kappa_1\alpha_1))} \tag{34}$$

where subscript i corresponds to the ith iteration of the four stages of one RK4 cycle, and $\nu_1=0$, $\nu_2=0.5$, $\nu_3=0.5$ and $\nu_4=1$. A similar expression is obtained for the $Q_2^{\sigma_{xy}}$ memory variable by swapping indices 1 and 2. The explicit, semi-implicit or implicit implementations of the auxiliary memory variables are obtained with $\theta=0$, 1/2 or 1 respectively. To illustrate more precisely how the velocity and stress components are calculated using the RK4 time scheme, the set T of variables (v_x, v_y, σ_{xx}, σ_{xy}, σ_{yy}) (see Figure 1) is updated at time step $n+1$ using T^n at time step n based on the following algorithm:

Let $T=T^n$; for $i=1$ to 4 do

$$\begin{aligned}\tilde{T} &= T^n+\nu_i\dot{T}^i\Delta t\\ \tilde{T} &= \tilde{T}+s((n+\nu_i)\Delta t)\\ \dot{T}^i &= f(\tilde{T},s^i)\\ T &= T+\pi_i\dot{T}^i\Delta t\end{aligned} \tag{35}$$

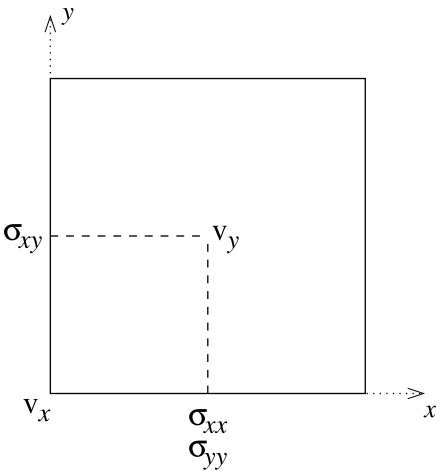

Figure 1: Elementary staggered finite-difference grid cell based on the components of the 2D velocity vector and stress tensor.

and then reset $T^{n+1} = T$ at the end of the cycle.

Function f represents the right-hand side of the velocity-stress equations (2) and is a function of the derivatives of the velocity and stress components, and of the known source term s. The constants of the RK4 scheme are $\nu_1 = 0$, $\nu_2 = 0.5$, $\nu_3 = 0.5$, $\nu_4 = 1$ and we also have $\pi_1 = 1/6$, $\pi_2 = 2/6$, $\pi_3 = 2/6$, $\pi_4 = 1/6$ (see Press, Teukolsky, Vetterling, and Flannery (1994)). In the case of a shift with only one pole, we set $\kappa_2 = 1$, $g_1 = 1$ and $Q_2^{\sigma_{xy}} = 0$ and then the high-order time discretization of equation (12) can be retrieved.

Instead of a classical Taylor expansion, we use the more accurate Holberg coefficients (Holberg, 1987; Rodrigues, 1993) to compute the spatial derivatives involved in the whole system of equations at eighth order in space. These coefficients are calculated by development and truncation at a given order and filtering so as to decrease the error made on the group velocity and therefore reduce the overall numerical dispersion. For instance the horizontal spatial derivative of a given variable V is computed numerically using

$$\frac{\partial V}{\partial x} \Big|_{i+1/2} = \frac{c_1(V_{i+1} - V_i) + c_2(V_{i+2} - V_{i-1}) + c_3(V_{i+3} - V_{i-2}) + c_4(V_{i+4} - V_{i-3})}{\Delta x} \quad (36)$$

where c_1 = +1.231666, c_2 = -0.1041182, c_3 = +0.02063707 and c_4 = -0.003570998.

4 Numerical results

To illustrate the equivalence of the CPML and ADE-PML formulations and also the good performance of ADE-PML at fourth order in time and eighth order in space, we perform several simulations in a homogeneous elastic medium with density $\rho = 2800$ kg.m^{-3}, pressure wave velocity $c_p = 3300$ m.s^{-1} and shear wave velocity $c_s = 1905$ m.s^{-1}. The domain has a size of 1000 m $\times$ 6400 m, including all the PML layers, and the numerical grid consists of 101 $\times$ 641 points with a 10 m spatial step. We perform the first two simulations with the classical CPML and the ADE-PML formulation with a second-order accurate solution method. The next two simulations are performed with the RK4 time-formulation and the 8th-order Holberg space-discretization with a single pole in the frequency shift, using first an explicit and second a semi-implicit ADE-PML time discretization. The time step is $\Delta t = 10^{-3}$ s to ensure stability based on the CFL stability condition of the explicit time schemes used. We compare the results to a reference solution computed with the same time step but on a larger grid. The source is the first derivative of a Gaussian in time with a dominant frequency of 8 Hz located at point ($x_s = 790$ m, $y_s = 4270$ m). The seismograms are recorded at three receivers located at points ($x_1 = 200$ m, $y_1 = 4130$ m), ($x_2 = 700$ m, $y_2 = 2270$ m) and ($x_3 = 810$ m, $y_3 = 270$ m). The first receiver is located close to the left PML at 100 m from its bottom, while the source and the second and third receivers are located very close to the right at around 200 m and 100 m respectively from the PML. The third receiver is located 4 km away from the source in order to analyze the impact of the PML on waves that travel a long distance at near grazing angles along the PML boundary. The configuration is shown in Figure 3.

For the sake of simplicity, we denote by RK4 the ADE-PML solution that involves one pole shift computed using a fourth-order Runge-Kutta time scheme and eighth-order space scheme with Holberg coefficients. To absorb the energy efficiently and avoid large reflections at grazing incidence, we take $\kappa_{max} = 1$, $\alpha_{max} = \pi f_0$ and d_{max} calculated as in Komatitsch and Martin (2007) with $R_c = 10^{-5}$. The PML layers have a thickness of 100 m, i.e., 10 grid points. In Figure 2, the seismograms of the horizontal and vertical components of the velocity vector calculated with second-order accurate CPML or second-order semi-implicit (or explicit) accurate ADE-PML show extremely similar behavior and are very well superimposed. The time evolution of total energy plotted in Figure 6 is also almost identical in the case of the second-order semi-implicit ADE-PML, which illustrates the equivalence of the CPML and ADE-PML techniques, the semi-implicit ADE-PML scheme showing an almost totally perfect agreement with CPML solutions in terms of total energy decay. This agreement is better than in the second-order explicit ADE-PML case.

In Figure 3 we show snapshots of wave propagation at different times using a

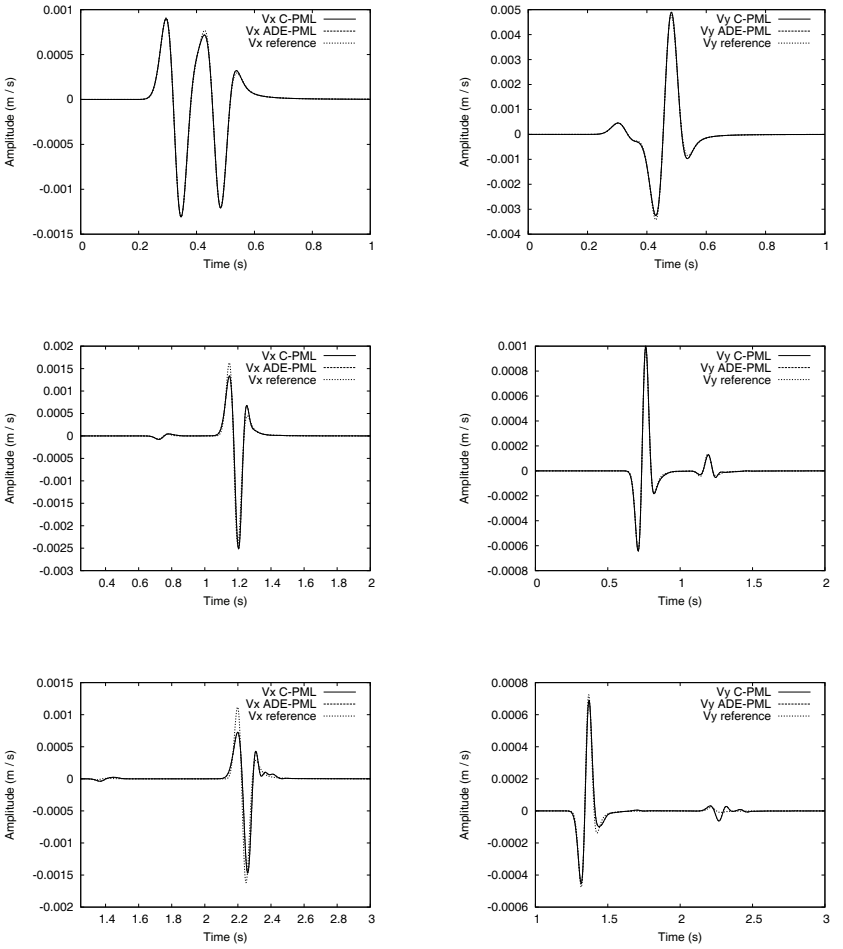

Figure 2: Second-order ADE-PML (dashed line) and classical CPML (solid line) solutions in a thin homogeneous elastic slice surrounded by four PMLs for the horizontal (left column) and vertical (right column) component of velocity recorded at the first (top), second (middle) and third (bottom) receivers (represented by green squares in Figure 3) compared to a reference solution (dotted line). At these receivers located close to the upper PML layers (10 grid points away from its beginning) the agreement is good in spite of the grazing incidence and almost no spurious oscillations are observed. The third receiver located far from the source exhibits more discrepancies because it is located at large offset and is therefore very sensitive to waves reaching the PML at very grazing incidence. ADE-PML and CPML are almost perfectly superimposed, which illustrates the equivalence between the two techniques. The differences appear mostly at medium and long time periods (Figure 6).

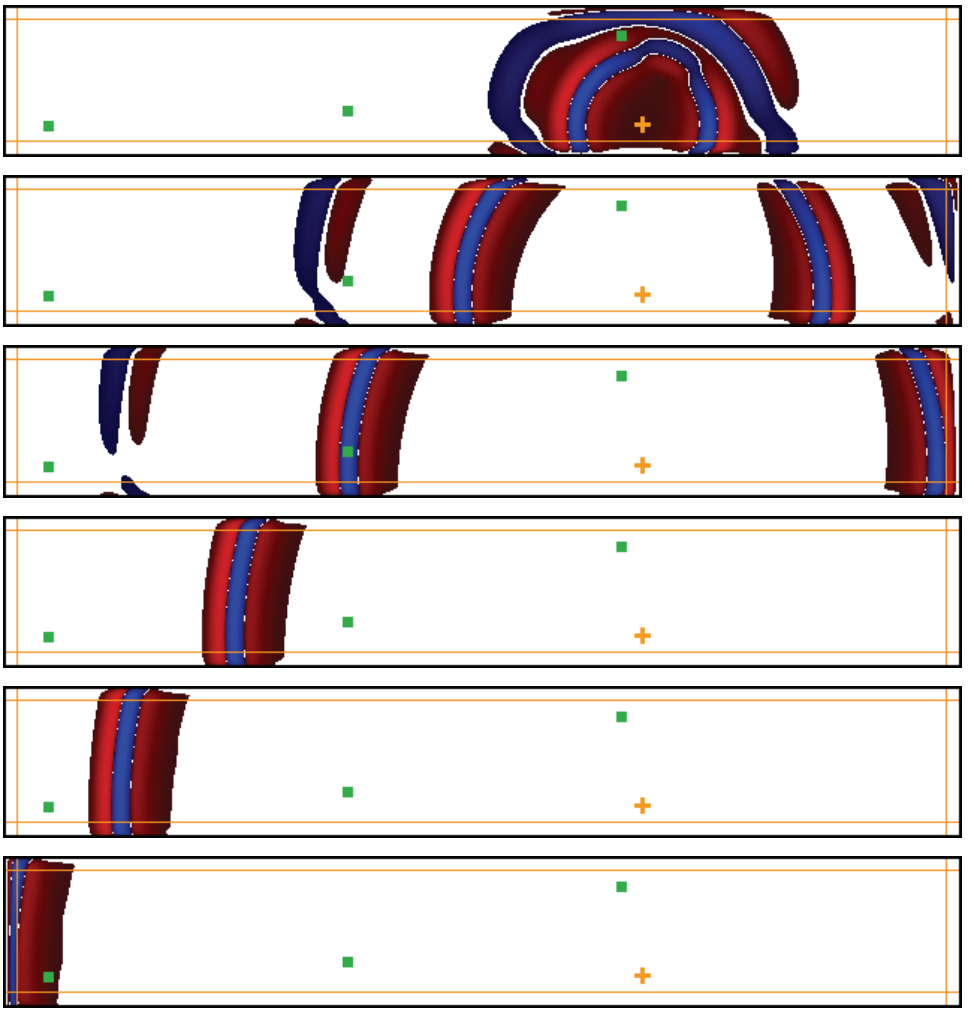

Figure 3: Snapshots of the horizontal component of the velocity vector in a homogeneous medium for a thin slice with ADE-PML conditions with $\alpha_{\max} = \pi f_0$ and $\kappa_{\max} = 1$ implemented on its four sides, at time 0.4 s (top), 0.8 s, 1.6 s, 2 s and 2.4 s (bottom). We represent it in red (positive) or blue (negative) when it has an amplitude higher than a threshold of 1% of the maximum, and the normalized value is raised to the power 0.30 to enhance small amplitudes that would otherwise not be clearly visible. The orange cross indicates the location of the source and the green squares the position of receivers at which seismograms are recorded. The four vertical or horizontal orange lines represent the edge of each PML layer. No spurious wave of significant amplitude is visible, even at grazing incidence. The snapshots have been rotated by 90° to fit on the page.

fourth-order Runge-Kutta time scheme. As in the case of the snapshots of second-order CPML shown in Figure 3 of Komatitsch and Martin (2007), no spurious modes propagate back into the main domain. Figure 4 shows comparisons between a reference solution and RK4 semi-implicit and explicit solutions. At the three receivers, RK4 simulations are far more accurate than the second order ADE-PML of Figure 2, which exhibits large discrepancies in terms of amplitude and spurious waves with larger errors at all the receivers, particularly at receiver #3 which is located far from the source and for which spurious waves have time to develop at grazing incidence. This is due to two main factors, the higher level of numerical dispersion of the second-order ADE-PML and the fact that the second-order ADE-PML is less accurate at a large offset close to the PML (which is similar as for the CPML seismograms shown in Komatitsch and Martin (2007)). In Figure 5, we show RK4 solutions computed with $\kappa_{max} = 7$. The results are improved at all receivers, even at receiver #3 at large offset, compared to solutions computed with $\kappa_{max} = 1$ in Figure 4. The explicit and semi-implicit solutions are still similar except in terms of decay of energy after approximately 5 s, when the physical waves have left the computational domain.

An important thing to study when designing a perfectly matched layer is the numerical stability of the PML at long time periods. In Figure 6, for a simulation over 10^6 time steps, we observe that in the first 3 s the total energy of the system decays much faster by almost 20 orders of magnitude using RK4 ADE-PMLs than using the second-order ADE-PML; and a semi-implicit scheme seems to ensure faster energy decay. Then, after around 5 s, energies computed with semi-implicit or explicit RK4 ADE-PML reach values as low as around 10^{-9} J (lower than the around 10^{-8} J reached in the second-order simulations) and values around 10^{-44} J and 10^{-46} J at around 100 s for the explicit and semi-implicit cases respectively, while in the case of the second-order ADE-PML total energy reaches values around 10^{-13} J at around 100 s. In all cases semi-implicit schemes show faster decay of energy.

In Figure 7 we compare RK4 simulations with two poles in the frequency shift to the reference solution. We take $\kappa_{1max} = 1$ and $\kappa_{2max} = 20$ with $\alpha_{1max} = \pi f_0$ and $\alpha_{2max} = 2\pi f_0$ but observe no significant improvement compared to the one-pole solution of Figure 4. For our seismic wave propagation application, using two poles is thus unnecessary and the one-pole version is sufficient to absorb the waves efficiently. In the case of Maxwell's equations, Gedney and Zhao (2010) mention that using two poles can be of interest when trying to damp evanescent waves, or in the case of periodic models, which is not the case for our seismic wave propagation application.

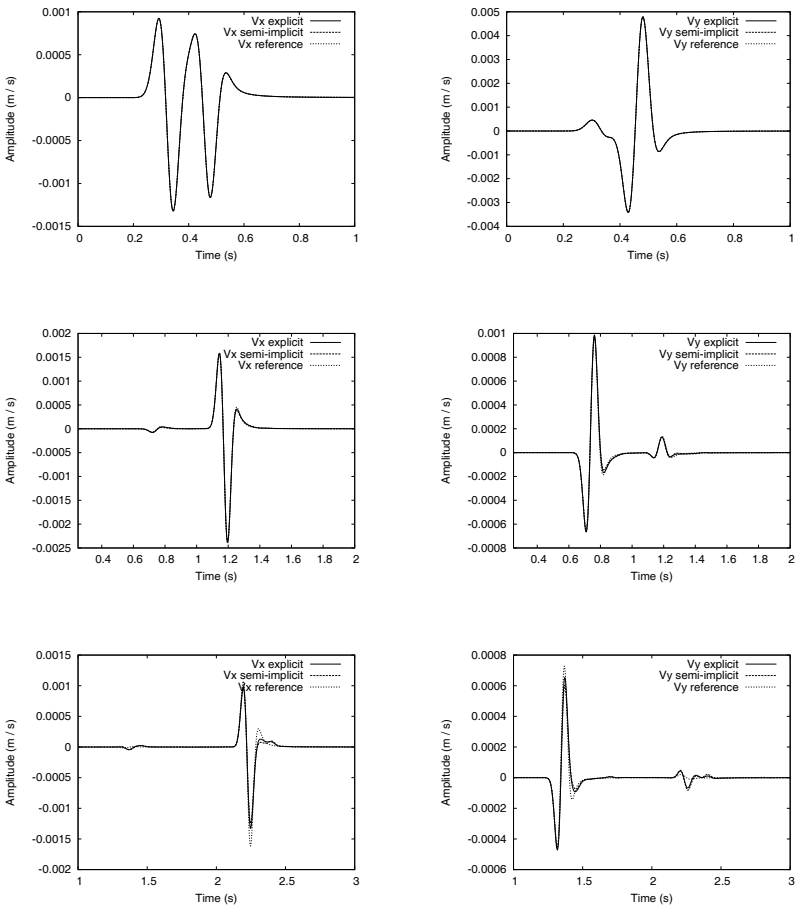

Figure 4: High-order (fourth-order in time and eighth-order in space) ADE-PML solution, using explicit or semi-implicit implementations of the auxiliary memory variables, in a thin homogeneous elastic slice surrounded by four PMLs for the horizontal (left column) and vertical (right column) component of the velocity vector recorded at the first (top), second (middle) and third (bottom) receiver (represented by green squares in Figure 3) compared to a reference solution (dotted line). At these receivers located close to the upper PML layers (10 grid points away from its beginning) the agreement is good in spite of the grazing incidence and almost no spurious oscillations are observed. The third receiver located far from the source exhibits more discrepancies because it is located at large offset and is therefore very sensitive to waves reaching the PML at very grazing incidence. The semi-implicit and explicit solutions are very similar and are more accurate than the second order solution shown in Figure 2. Semi-implicit or explicit ADE-PML and reference solutions are almost perfectly superimposed, which illustrates the good accuracy of ADE-PML. The differences between semi-implicit and explicit techniques appear mostly at medium and long time periods (Figure 6).

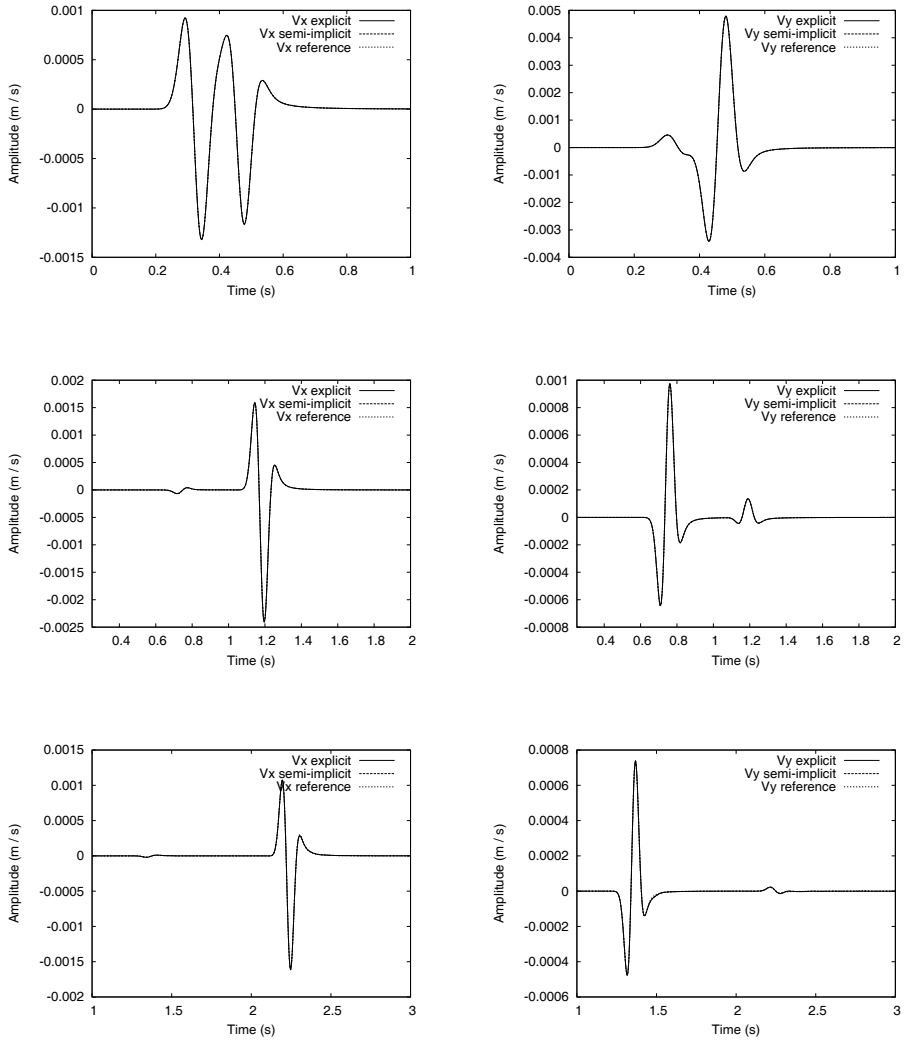

Figure 5: Same as in Figure 4 but with $\kappa_{max} = 7$ instead of $\kappa_{max} = 1$. At these receivers located close to the PML layers (10 grid points away from its beginning) the agreement is good in spite of the grazing incidence and only tiny spurious oscillations are observed. At the third receiver the improvement is particularly significant compared to Figure 4. The semi-implicit and explicit solutions are very similar and are more accurate than the second-order solution of Figure 2 and the high-order solution of Figure 4.

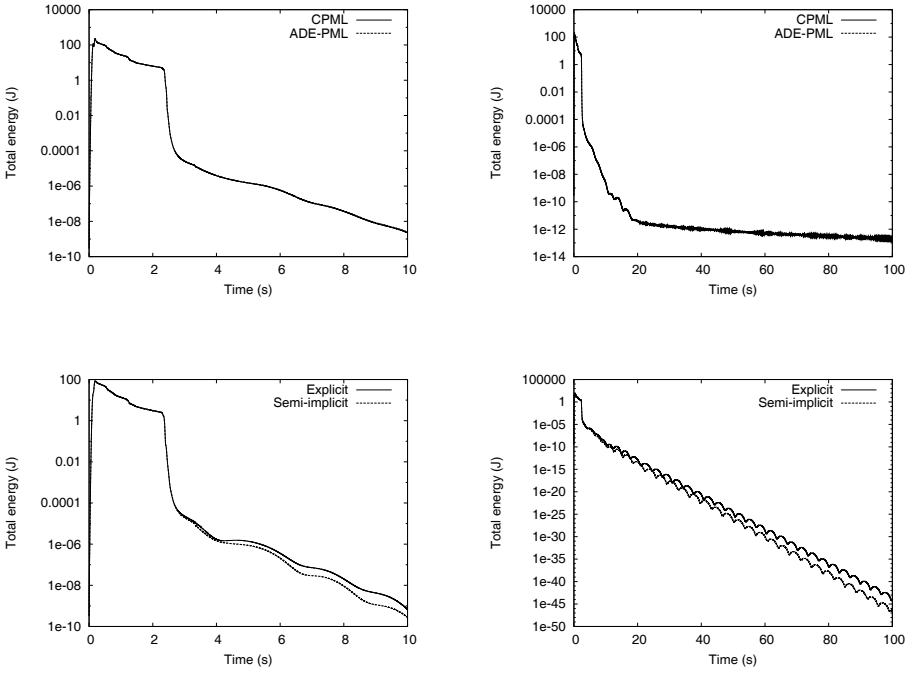

Figure 6: (Top): Decay with time of total energy in semi-logarithmic scale for the homogeneous elastic medium modeled in the seismograms of Figure 2 and the snapshots of Figure 3 for medium and long time periods, up to 100 s (i.e. 100,000 time steps) of simulation for the second-order CPML (dashed line) and second-order ADE-PML (solid line). Both energy curves are superimposed, which illustrates again the equivalence of the two formulations. No instabilities appear even at long time periods where energy values as low as 10^{-13}J are reached. (Bottom): Energy decay for medium and long time periods (100 s, i.e. 100,000 time steps) for the numerical solution of Figure 4. No instabilities are observed in the explicit or semi-implicit high-order RK4 solutions, which means that the discrete ADE-PML at the fourth order in time and eighth order in space is stable up to 100,000 time steps. Total energy reaches a value as low as 10^{-9} J at $t = 5$ s, while it reaches a value of 10^{-8} J in the second-order case (top). After 100 s total energy is 10^{-44} J in the explicit case and 10^{-46}J in the semi-implicit case, while it is around 10^{-13} J in the second-order case (top). The semi-implicit case seems to lead to faster decay of the energy in all cases.

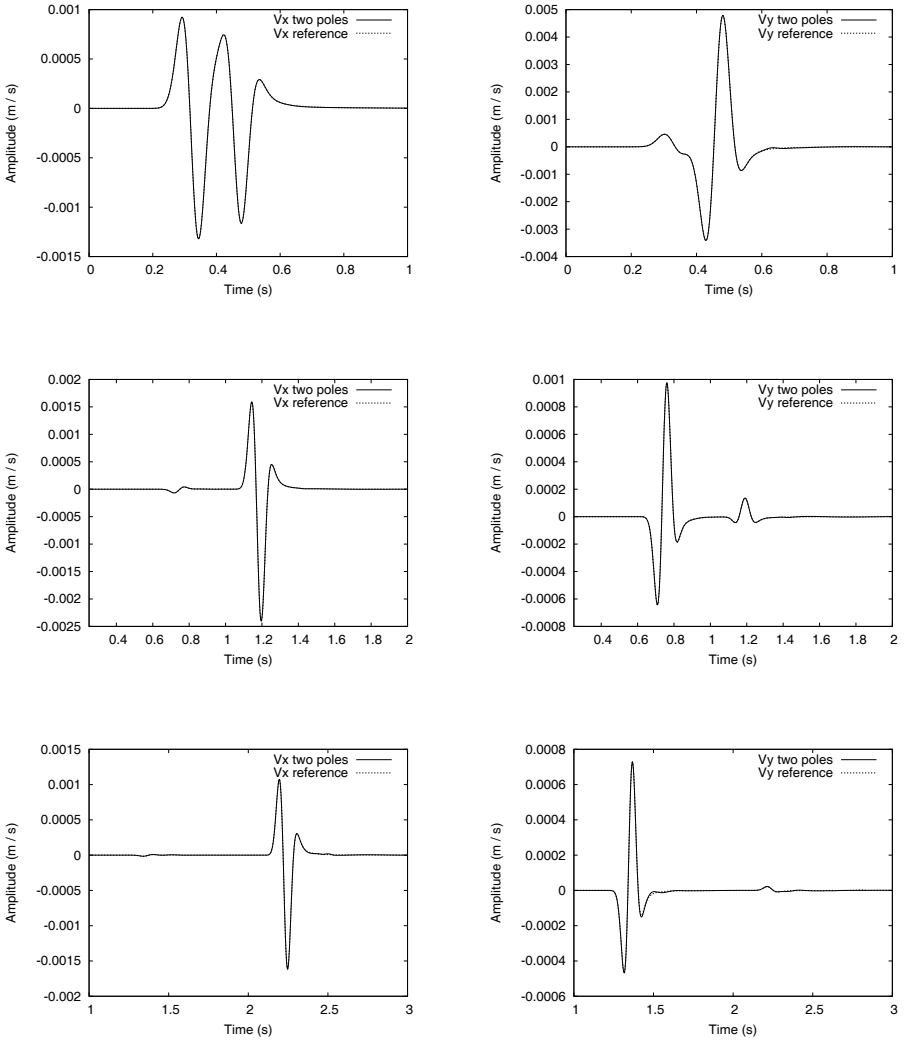

Figure 7: Same as in Figure 5 but with two poles in the frequency shift, and using $\kappa_{1max} = 1$ and $\kappa_{2max} = 20$ instead of $\kappa_{max} = 7$ in the one-pole case. No significant improvement is observed compared to the one-pole solution of Figure 5.

5 Conclusions

We have shown that at the second order in time the convolutional PML can be derived from a more general non-convolutional ADE-PML formulation. To increase accuracy we then designed a non-convolutional ADE-PML optimized at grazing incidence that can be generalized to high-order schemes in time and that is numerically stable up to 100,000 time steps. Long time stability is ensured numerically with RK4 ADE-PML, as in the classical second-order CPML and also the second-order ADE-PML, but solutions are more accurate.

We have implemented semi-implicit and explicit time schemes for the auxiliary memory variables and have shown that a semi-implicit scheme leads to more efficient energy absorption at long time duration in all cases. If the value of κ_{max} is increased from 1 to 7, solutions are improved at large offset and at grazing incidence. As mentioned in Martin and Komatitsch (2009), in practice one can not use a value of κ_{max} much higher than around 20 because otherwise steep variations of the $\kappa(x)$ profile are not accurately discretized by the numerical grid.

Finally, at high order in time and space the one-pole version of ADE-PML is sufficient to ensure accurate results in our application, and the more general two-pole version does not bring significant improvements in terms of accuracy.

Acknowledgement: The authors thank Heiner Igel and Peter Moczo for fruitful discussions about high-order time schemes for finite-difference techniques.

References

Basu, U. (2009): Explicit finite-element perfectly matched layer for transient three-dimensional elastic waves. *Int. J. Numer. Meth. Eng.*, vol. 77, pp. 151–176.

Basu, U.; Chopra, A. K. (2004): Perfectly matched layers for transient elastodynamics of unbounded domains. *Int. J. Numer. Meth. Eng.*, vol. 59, pp. 1039–1074.

Bérenger, J. P. (1994): A Perfectly Matched Layer for the absorption of electromagnetic waves. *J. Comput. Phys.*, vol. 114, pp. 185–200.

Bérenger, J. P. (2002): Application of the CFS PML to the absorption of evanescent waves in waveguides. *IEEE Microwave and Wireless Components Letters*, vol. 12, no. 6, pp. 218–220.

Bérenger, J. P. (2002): Numerical reflection from FDTD-PMLs: A comparison of the split PML with the unsplit and CFS PMLs. *IEEE Transactions on Antennas and Propagation*, vol. 50, no. 3, pp. 258–265.

Cerjan, C.; Kosloff, D.; Kosloff, R.; Reshef, M. (1985): A nonreflecting boundary condition for discrete acoustic and elastic wave equation. *Geophysics*, vol. 50, pp. 705–708.

Chaljub, E.; Komatitsch, D.; Vilotte, J. P.; Capdeville, Y.; Valette, B.; Festa, G. (2007): Spectral element analysis in seismology. In Wu, R.-S.; Maupin, V.(Eds): *Advances in wave propagation in heterogeneous media*, volume 48 of *Advances in Geophysics*, pp. 365–419. Elsevier - Academic Press.

Chew, W. C.; Liu, Q. (1996): Perfectly Matched Layers for elastodynamics: a new absorbing boundary condition. *J. Comput. Acoust.*, vol. 4, no. 4, pp. 341–359.

Chew, W. C.; Weedon, W. H. (1994): A 3-D perfectly matched medium from modified Maxwell's equations with stretched coordinates. *Microwave Opt. Technol. Lett.*, vol. 7, no. 13, pp. 599–604.

Cohen, G.; Fauqueux, S. (2005): Mixed spectral finite elements for the linear elasticity system in unbounded domains. *SIAM Journal on Scientific Computing*, vol. 26, no. 3, pp. 864–884.

Collino, F.; Monk, P. (1998): Optimizing the Perfectly Matched Layer. *Comput. Meth. Appl. Mech. Eng.*, vol. 164, pp. 157–171.

Collino, F.; Tsogka, C. (2001): Application of the PML absorbing layer model to the linear elastodynamic problem in anisotropic heterogeneous media. *Geophysics*, vol. 66, no. 1, pp. 294–307.

Dablain, M. A. (1986): The application of high-order differencing to the scalar wave equation. *Geophysics*, vol. 51, no. 1, pp. 54–66.

Drossaert, F. H.; Giannopoulos, A. (2007): A nonsplit complex frequency-shifted PML based on recursive integration for FDTD modeling of elastic waves. *Geophysics*, vol. 72, no. 2, pp. T9–T17.

Engquist, B.; Majda, A. (1977): Absorbing boundary conditions for the numerical simulation of waves. *Math. Comp.*, vol. 31, pp. 629–651.

Fauqueux, S. (2003): *Eléments finis mixtes spectraux et couches absorbantes parfaitement adaptées pour la propagation d'ondes élastiques en régime transitoire*. PhD thesis, Université Paris-Dauphine, Paris, France, 2003.

Festa, G.; Delavaud, E.; Vilotte, J. P. (2005): Interaction between surface waves and absorbing boundaries for wave propagation in geological basins: 2D numerical simulations. *Geophys. Res. Lett.*, vol. 32, no. 20, pp. L20306.

Festa, G.; Vilotte, J. P. (2005): The Newmark scheme as velocity-stress time-staggering: an efficient PML implementation for spectral-element simulations of elastodynamics. *Geophys. J. Int.*, vol. 161, pp. 789–812.

Gedney, S. D.; Zhao, B. (2010): An auxiliary differential equation formulation for the complex-frequency shifted PML. *IEEE Transactions on Antennas and Propagation*, vol. 58, no. 3, pp. 838–847.

Givoli, D. (1991): Non-reflecting boundary conditions: review article. *J. Comput. Phys.*, vol. 94, pp. 1–29.

Givoli, D. (2008): Computational absorbing boundaries. In Marburg, S.; Nolte, B.(Eds): *Computational acoustics noise propagation in fluids*, volume 5, pp. 145–166. Springer-Verlag, Berlin, Germany.

Hagstrom, T.; Hariharan, S. I. (1998): A formulation of asymptotic and exact boundary conditions using local operators. *Appl. Num. Math.*, vol. 27, pp. 403–416.

Higdon, R. L. (1991): Absorbing boundary conditions for elastic waves. *Geophysics*, vol. 56, pp. 231–241.

Holberg, O. (1987): Computational aspects of the choice of operator and sampling interval for numerical differentiation in large-scale simulation of wave phenomena. *Geophys. Prospect.*, vol. 35, pp. 629–655.

Kawase, H. (1988): Time-domain response of a semi-circular canyon for incident *SV*, *P* and Rayleigh waves calculated by the discrete wavenumber boundary element method. *Bull. Seismol. Soc. Am.*, vol. 78, pp. 1415–1437.

Komatitsch, D.; Coutel, F.; Mora, P. (1996): Tensorial formulation of the wave equation for modelling curved interfaces. *Geophys. J. Int.*, vol. 127, no. 1, pp. 156–168.

Komatitsch, D.; Martin, R. (2007): An unsplit convolutional Perfectly Matched Layer improved at grazing incidence for the seismic wave equation. *Geophysics*, vol. 72, no. 5, pp. SM155–SM167.

Komatitsch, D.; Tromp, J. (2003): A Perfectly Matched Layer absorbing boundary condition for the second-order seismic wave equation. *Geophys. J. Int.*, vol. 154, no. 1, pp. 146–153.

Kristek, J.; Moczo, P.; Galis, M. (2009): A brief summary of some PML formulations and discretizations for the velocity-stress equation of seismic motion. *Studia Geophysica et Geodaetica*, vol. 53, no. 4, pp. 459–474.

Kuzuoglu, M.; Mittra, R. (1996): Frequency dependence of the constitutive parameters of causal perfectly matched anisotropic absorbers. *IEEE Microwave and Guided Wave Letters*, vol. 6, no. 12, pp. 447–449.

Liu, Q.; Polet, J.; Komatitsch, D.; Tromp, J. (2004): Spectral-element moment tensor inversions for earthquakes in Southern California. *Bull. Seismol. Soc. Am.*, vol. 94, no. 5, pp. 1748–1761.

Lu, Y. Y.; Zhu, J. (2007): Perfectly matched layer for acoustic waveguide modeling - Benchmark calculations and perturbation analysis. *CMES: Computer Modeling in Engineering and Sciences*, vol. 22, no. 3, pp. 235–248.

Luebbers, R. J.; Hunsberger, F. (1992): FDTD for Nth-order dispersive media. *IEEE Transactions on Antennas and Propagation*, vol. 40, no. 11, pp. 1297–1301.

Lysmer, J.; Drake, L. A. (1972): A finite element method for seismology. In Alder, B.; Fernbach, S.; Bolt, B. A.(Eds): *Methods in Computational Physics*, volume 11, chapter 6, pp. 181–216. Academic Press, New York, USA.

Ma, S.; Liu, P. (2006): Modeling of the perfectly matched layer absorbing boundaries and intrinsic attenuation in explicit finite-element methods. *Bull. Seismol. Soc. Am.*, vol. 96, no. 5, pp. 1779–1794.

Madariaga, R. (1976): Dynamics of an expanding circular fault. *Bull. Seismol. Soc. Am.*, vol. 66, no. 3, pp. 639–666.

Marcinkovich, C.; Olsen, K. B. (2003): On the implementation of perfectly matched layers in a three-dimensional fourth-order velocity-stress finite-difference scheme. *J. Geophys. Res.*, vol. 108, no. B5, pp. 2276.

Martin, R.; Komatitsch, D. (2006): An optimized convolution-perfectly matched layer (C-PML) absorbing technique for 3D seismic wave simulation based on a finite-difference method. *Geophysical Research Abstracts*, vol. 8, pp. 03988. Abstract EGU06-A-03988, www.cosis.net/abstracts/EGU06/03988/EGU06-J-03988-1.pdf.

Martin, R.; Komatitsch, D. (2009): An unsplit convolutional perfectly matched layer technique improved at grazing incidence for the viscoelastic wave equation. *Geophys. J. Int.*, vol. 179, no. 1, pp. 333–344.

Martin, R.; Komatitsch, D.; Barucq, H. (2005): An optimized convolution-perfectly matched layer (C-PML) absorbing technique for 3D seismic wave simulation based on a finite-difference method. *Eos Trans. AGU*, vol. 86, no. 52, pp. Fall Meet. Suppl., Abstract NG43B–0574. www.agu.org/meetings/fm05/waisfm05.html.

Martin, R.; Komatitsch, D.; Ezziani, A. (2008): An unsplit convolutional perfectly matched layer improved at grazing incidence for seismic wave equation in poroelastic media. *Geophysics*, vol. 73, no. 4, pp. T51–T61.

Martin, R.; Komatitsch, D.; Gedney, S. D. (2008): A variational formulation of a stabilized unsplit convolutional perfectly matched layer for the isotropic or

anisotropic seismic wave equation. *CMES: Computer Modeling in Engineering and Sciences*, vol. 37, no. 3, pp. 274–304.

Meza-Fajardo, K. C.; Papageorgiou, A. S. (2008): A nonconvolutional, split-field, perfectly matched layer for wave propagation in isotropic and anisotropic elastic media: Stability analysis. *Bull. Seismol. Soc. Am.*, vol. 98, no. 4, pp. 1811–1836.

Moczo, P.; Robertsson, J.; Eisner, L. (2007): The finite-difference time-domain method for modeling of seismic wave propagation. In Wu, R.-S.; Maupin, V.(Eds): *Advances in wave propagation in heterogeneous media*, volume 48 of *Advances in Geophysics*, chapter 8, pp. 421–516. Elsevier - Academic Press.

Press, W. H.; Teukolsky, S. A.; Vetterling, W. T.; Flannery, B. P. (1994): *Numerical recipes: the art of scientific computing*. Cambridge University Press, Cambridge, USA.

Roden, J. A.; Gedney, S. D. (2000): Convolution PML (CPML): An efficient FDTD implementation of the CFS-PML for arbitrary media. *Microwave and Optical Technology Letters*, vol. 27, no. 5, pp. 334–339.

Rodrigues, D. (1993): *Simulation de la propagation d'ondes sismiques sur machine massivement parallèle*. PhD thesis, École Centrale de Paris, Paris, France, 1993.

Rodríguez-Castellanos, A.; Sánchez-Sesma, F.; Luzón, F.; Martin, R. (2006): Multiple scattering of elastic waves by subsurface fractures and cavities. *Bull. Seismol. Soc. Am.*, vol. 96, no. 4A, pp. 1359–1374.

Sánchez-Sesma, F. J.; Campillo, M. (1991): Diffraction of *P*, *SV* and Rayleigh waves by topographic features: a boundary integral formulation. *Bull. Seismol. Soc. Am.*, vol. 81, pp. 2234–2253.

Sochacki, J.; Kubichek, R.; George, J.; Fletcher, W. R.; Smithson, S. (1987): Absorbing boundary conditions and surface waves. *Geophysics*, vol. 52, no. 1, pp. 60–71.

Stacey, R. (1988): Improved transparent boundary formulations for the elastic wave equation. *Bull. Seismol. Soc. Am.*, vol. 78, no. 6, pp. 2089–2097.

Tessmer, E.; Kosloff, D. (1994): 3-D elastic modeling with surface topography by a Chebyshev spectral method. *Geophysics*, vol. 59, no. 3, pp. 464–473.

Tromp, J.; Komatitsch, D.; Liu, Q. (2008): Spectral-element and adjoint methods in seismology. *Communications in Computational Physics*, vol. 3, no. 1, pp. 1–32.

Virieux, J. (1986): *P-SV* wave propagation in heterogeneous media: velocity-stress finite-difference method. *Geophysics*, vol. 51, pp. 889–901.

Wang, T.; Tang, X. (2003): Finite-difference modeling of elastic wave propagation: A nonsplitting perfectly matched layer approach. *Geophysics*, vol. 68, no. 5, pp. 1749–1755.

Zeng, Y. Q.; He, J. Q.; Liu, Q. H. (2001): The application of the perfectly matched layer in numerical modeling of wave propagation in poroelastic media. *Geophysics*, vol. 66, no. 4, pp. 1258–1266.